DOI: 10.1021/ma902712u

Macromolecules
ARTICLE

Formation of Side-Chain Hetero-Polypseudorotaxane Composed of α- and β-Cyclodextrins with a Water-Soluble Polymer Bearing Two Recognition Sites

Daisuke Taura,[†] Shujing Li,[†] Akihito Hashidzume,[†] and Akira Harada*[,†,‡]

[†]*Department of Macromolecular Science, Graduate School of Science, Osaka University, 1-1 Machikaneyama-cho, Toyonaka, Osaka 560-0043, Japan and* [‡]*Core Research for Evolutional Science and Technology (CREST), Japan Science and Technology Agency (JST), 5 Sanban-cho, Chiyoda-ku, Tokyo 102-0075, Japan*

Received December 9, 2009; Revised Manuscript Received January 10, 2010

ABSTRACT: A side-chain hetero-polypseudorotaxane was prepared from a water-soluble polymer (**1**) bearing heptamethylene (C_7) and azobenzene (Azo) moieties connected with oligo(ethylene glycol) in the side chain by three steps, in which α- and β-cyclodextrins (α- and β-CDs) included the C_7 and *cis*-Azo moieties, respectively. In the first step, α-CD was added to **1** to form the side-chain polypseudorotaxane, in which α-CD included both the C_7 and *trans*-Azo moieties in the side chain. In the second step, the Azo moiety at the end of the side chain was isomerized to the *cis* isomer to form the side-chain polyrotaxane, in which α-CD was interlocked on the side chain. In the final step, β-CD was added to the side-chain polyrotaxane to form the side-chain hetero-polypseudorotaxane.

Introduction

Biological systems maintain living activities utilizing well-sophisticated macromolecular assemblies, e.g., ATP synthase, myosin and actin, kinesin and dynein microtubules, and microfilaments, as supramolecular machines.[1] These biological supramolecular machines have inspired a number of research groups to study aiming at the construction of highly functional artificial supramolecular machines.[2] One of important building units of artificial supramolecular machines is a rotaxane, in which a rotor molecule is mechanically interlocked on an axis molecule by bulky stoppers at the ends of the axis.[3−5] A number of examples of supramolecular machines bearing rotaxane units have been reported, for example, "a molecular elevator" by Stoddart et al.[6] and "a molecular information ratchet" by Leigh et al.[7] Recently, molecular muscles have attracted increasing interest from researchers utilizing doubly threaded rotaxanes because of nanotechnological applications.[8] Sauvage et al.[9] synthesized a rotaxane dimer containing two Cu(I) metals and two identical ring-and-string components, which performed the contraction and expansion movements by the extraction of Cu(I) with KCN and by the remetalation with Zn(II). More recently, Stoddart et al.[10] reported the construction of the system for the expansion and contraction movements of the polymeric [*c*2]daisy chains consisting of crown ether and ammonium moieties, which was responsive to acid and base conditions. Grubbs et al.[11] also reported pH-responsive size changes of a polymer of doubly threaded dimer units consisting of crown ether and ammonium moieties linked by "click chemistry".

Most of examples described above dealt with crown ether derivatives as rotor molecules. On the other hand, from the viewpoint of the environmental consideration, we have been focused on cyclodextrin (CD) as a rotor component, which can be utilized in aqueous media. We have synthesized and reported various supramolecular polymers including main-chain and side-chain polypseudorotaxanes and polyrotaxanes.[12−14]

*Corresponding author: Fax +81-6-6850-5445; e-mail harada@chem.sci.osaka-u.ac.jp.

One of previous studies demonstrated that the doubly threaded α-CD dimer composed of a longer alkyl chain exhibited the contraction movement by changing solvent polarity.[15,16] In these systems, two recognition sites are located close to each other. In order to obtain large size changes, it is necessary to separate two recognition sites with a longer linker. Recently, we have prepared an α-CD derivative composed of photoresponsive and nonresponsive sites connected with oligo(ethylene glycol) (OEG) and constructed the size changes in hydrodynamic radius of the doubly threaded dimer by the photoisomerization.[17] This compound is one of great promising building blocks not only for the main-chain linear stretching polymers by reacting both the ends but also for the side-chain stretching polymers by cross-linking polymer chains.

Another possibility to construct the stretching polymers is the systems consisting of polymers which bear two recognition sites linked with a longer linker and CD, respectively, in their side chains. In this study, we have synthesized a water-soluble polymer (**1** in Scheme 1B) bearing heptamethylene (C_7) and azobenzene (Azo) moieties connected with a longer OEG, which act as recognition sites. Herein, for achieving the contraction and expansion systems, we report the preliminary data concerning the investigation of the side-chain hetero-polypseudorotaxane composed of α- and β-CDs, which stay at the C_7 and Azo moieties, respectively, by the stepwise preparation utilizing the isomerization of the photoresponsive Azo moiety.[18]

Experimental Section

Materials. Dichloromethane (DCM), diethyl ether (Et_2O), dimethylformamide (DMF), tetrahydrofuran (THF), and toluene were purified by utilizing a Glass Contour solvent dispending system. Oligo(ethylene glycol) (OEG, MW = 1.0×10^3) was purchased from NOF Corp. α-Cyclodextrin and β-cyclodextrin (α-CD and β-CD) were recrystallized from water. Water used for dialysis was purified with a Millipore Milli-Q system. Other reagents were used without further purification.

 Published on Web 01/20/2010

Scheme 1. Preparation of a Water-Soluble Polymer (1)

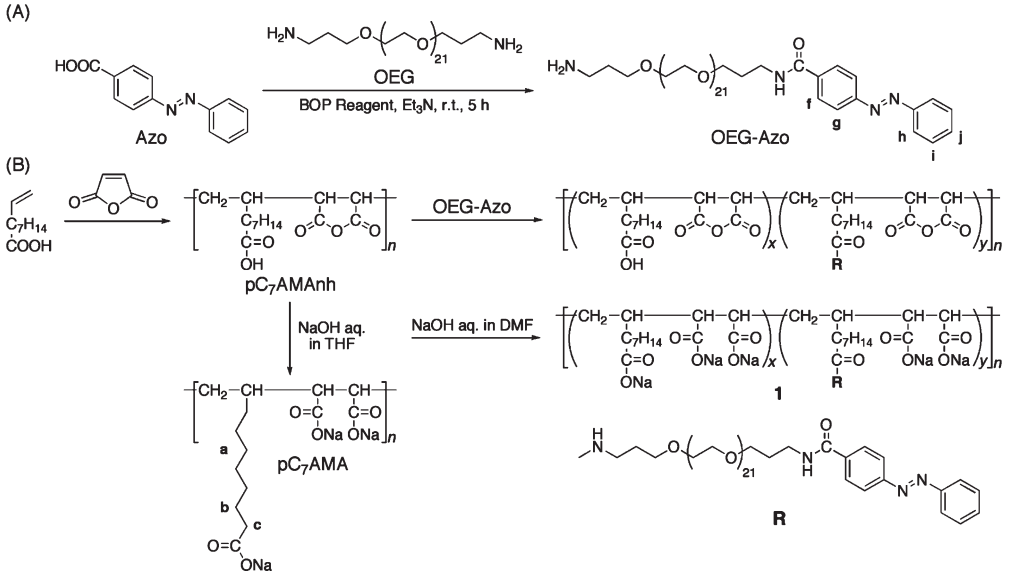

Preparation of *N*-(3-(2-(3-Aminopropoxy)oligoethoxy)propyl)-4-(phenyldiazenyl)benzamide (OEG-Azo). The synthetic scheme of OEG-Azo is shown in Scheme 1A. 4-(Phenylazo)benzoic acid (0.567 g, 2.51 mmol) and 1*H*-benzotriazol-1-yloxytripyrrolidinophosphonium hexafluorophosphate (BOP reagent, 1.95 g, 3.75 mmol) were suspended in DCM (120 mL). The suspended solution was added into a solution of OEG (2.61 g, 2.50 mmol) and triethylamine (Et_3N, 1.05 mL, 7.54 mmol) in DCM (60 mL). After stirring for 5 h at ambient temperature, the solvent and Et_3N were removed by evaporation and the crude product was dried under vacuum at 60 °C. The product was purified by liquid chromatography/mass spectrometry (LC/MS) using a mixed solvent of water and methanol as eluent. The orange viscous product was obtained in a 18.5% yield (0.578 g). ^{1}H NMR (500 MHz, DMSO, 30 °C): 8.60 (t, 1H, amide), 8.05 (td, 2H, azobenzene), 7.96−7.92 (m, 4H, azobenzene), 7.65−7.59 (m, 2H, azobenzene), 2.80 (t, 2H, methylene), 1.79 (quin, 2H, methylene), 1.72 (quin, 2H, methylene). Positive ion MALDI-TOF MS (*n*: the number of ethylene glycol unit in OEG moiety) *m*/*z* 1156.4 [M (*n* = 21) + K]$^+$, 1200.5 [M (*n* = 22) + K]$^+$, 1244.5 [M (*n* = 23) + K]$^+$, 1288.5 [M (*n* = 24) + K]$^+$, 1332.5 [M (*n* = 25) + K]$^+$, 1376.5 [M (*n* = 26) + K]$^+$, 1420.5 [M (*n* = 27) + K]$^+$, 1464.6 [M (*n* = 28) + K]$^+$, 1508.5 [M (*n* = 29) + K]$^+$, 1552.5 [M (*n* = 30) + K]$^+$, 1596.5 [M (*n* = 31) + K]$^+$, 1640.5 [M (*n* = 32) + K]$^+$, 1684.8 [M (*n* = 33) + K]$^+$, 1728.5 [M (*n* = 34) + K]$^+$, 1772.6 [M (*n* = 35) + K]$^+$.

Preparation of the Water-Soluble Polymer (1). The water-soluble polymer (**1**) was prepared according to Scheme 1B. 9-Decenoic acid (2.0 g, 0.012 mol), maleic anhydride (1.2 g, 0.012 mol), and 2,2′-azoisobutyronitrile (AIBN) (9.8 mg, 0.060 mmol) were added into a Schlenk flask and dried under vacuum. Then, these compounds were dissolved in toluene (3.0 mL) under a nitrogen atmosphere at ambient temperature. The Schlenk flask was immersed in an oil bath thermostated at 70 °C. After stirring for 18 h, the viscous precipitate was dissolved in THF. The polymer was precipitated by pouring the THF solution into a large amount of Et_2O and washed with Et_2O. After collecting by centrifugation, the polymer was dried under vacuum. The polymer obtained was purified by reprecipitation three times. The polymer (pC_7AMAnh) was obtained in a 38% yield (1.2 g). The number-average molecular weight (M_n) and the ratio of weight to number-average molecular weights (M_w/M_n) of the polymer were determined to be 1.1×10^4 and 3.1, respectively, by gel permeation chromatography (GPC) for the esterified sample of pC_7AMAnh using diazomethane.

The polymer (pC_7AMAnh, 64.5 mg, 0.240 mmol), *N*,*N*′-dicyclohexylcarbodiimide (74.3 mg, 0.360 mmol), and 1-hydroxybenzotriazole (48.6 mg, 0.360 mmol) were added into a Schlenk flask and dried under vacuum. Then, these compounds were dissolved in DMF (2.0 mL) under a nitrogen atmosphere, and the Schlenk flask was immersed in an ice bath. After stirring for 1 h, OEG-Azo (300 mg, 0.240 mmol) was dissolved in the DMF solution under a nitrogen atmosphere. After stirring for 3 days at ambient temperature, the insoluble dicyclohexylurea was removed by centrifugation, and the solvent of the supernatant solution was evaporated. The crude product was dried under vacuum at 60 °C. Furthermore, the crude product was dissolved in DMF and hydrolyzed with an excess of 0.50 M aqueous sodium hydroxide. After stirring at ambient temperature, the solvents were evaporated and the crude product was dried under vacuum at 60 °C. The crude product was purified by dialysis (molecular weight cutoff: 2000) against pure water for a week. The orange sticky polymer (**1**) was obtained in a 39.2% yield (147 mg) after recovering by freeze-drying. The content of OEG-Azo modified with the polymer side chain was roughly estimated to be 59 mol % by ^{1}H NMR.

Preparation of the Model Polymer (pC_7AMA). The model polymer (pC_7AMA) was prepared as shown in Scheme 1B. The polymer (pC_7AMAnh, 54.3 mg, 0.202 mmol) obtained was hydrolyzed with 0.50 M aqueous sodium hydroxide (5.0 mL, 2.5 mmol) in THF (1.0 mL). The hydrolyzed white polymer (pC_7AMA) obtained was purified by dialysis (molecular weight cutoff: 1000) against pure water for 4 days and recovered by freeze-drying in a 89.2% yield (62.9 mg).

Photoisomerization of the Azo Moiety. The samples used in this study were isomerized by photoirradiation using an Asahi Spectra compact xenon light source MAX-302 equipped with an HQBP 365 (Asahi Spectra Co.) band-pass filter (wavelength = 365 ± 10 nm). The distance between the sample and the light source was fixed at ca. 0.4 cm.

General Measurements. Positive-ion matrix-assisted laser desorption/ionization time-of-flight (MALDI-TOF) mass spectrometry experiments were performed using a Shimadzu/KRATOS Axima CFR Ver.2.2.3 mass spectrometer calibrated by α-cyano-4-hydroxycinnamic acid and insulin.

LC/MS experiments were carried out on Waters 2545 and Waters 515 as the binary and makeup pumps equipped with SunFire Prep C18 OBD column (19 × 150 mm), using the gradient program of water and methanol as eluent at a flow rate of 10 mL/min. Waters SFO and Waters 2767 were used as the switching valve and injector/fraction collector. A Waters

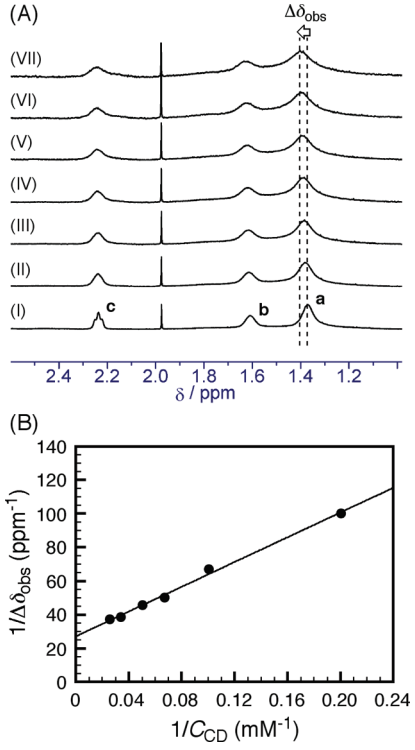

Figure 1. ^{1}H NMR spectra (A) of 1.0 mM pC$_7$AMA (I) in the presence of various concentrations (C_{CD}) of α-CD measured in D_2O containing 5.0 mM $NaHCO_3$ and 5.0 mM Na_2CO_3 at 30 °C. C_{CD}: 0 (I), 5.0 (II), 10.0 (III), 15.0 (IV), 20.0 (V), 30.0 (VI), and 40.0 mM (VII). Benesi−Hildebrand plot (B) of $1/\Delta\delta_{obs}$ against $1/C_{CD}$.

3100 mass detector and Waters 2996 photodiode array detector were also used as MS and UV detectors. The LC, MS, and mass-directed fraction collection were controlled by Masslynx version 4.1 with Fractionlynax.

GPC analysis was carried out at 40 °C on a Tosoh CCP & 8010 system equipped with two Tosoh TSKgel MultiporeH$_{XL}$-M columns connected in series, using THF as eluent at a flow rate of 0.8 mL/min. Tosoh UV-8010 and Tosoh RI-8012 detectors were used. The molecular weights were calibrated by polystyrene standards (Tosoh TSK polystyrene standard).

^{1}H NMR spectra were measured on a JEOL ECA500 NMR spectrometer at 30 °C. 2D NOESY data were obtained on a Varian UNITY INOVA plus 600 spectrometer at 30 °C. In the 2D NOESY NMR, the mixing time before the acquisition of free induction decay was fixed at 200 ms for all the samples. For all the NMR measurements, D_2O containing 5.0 mM $NaHCO_3$ and 5.0 mM Na_2CO_3 was used as a solvent. Tetramethylammonium chloride was used as an internal standard to determine chemical shifts.

UV−vis absorption spectra were recorded on a JASCO V-650 spectrometer in D_2O containing 5.0 mM $NaHCO_3$ and 5.0 mM Na_2CO_3 at 30 °C with 1 cm quartz cell.

Circular dichroism (cd) spectra were recorded on a JASCO J-820 spectrometer in D_2O containing 5.0 mM $NaHCO_3$ and 5.0 mM Na_2CO_3 at 30 °C with 1 cm quartz cell.

Results and Discussion

Estimation of Association Constants (*K*) for α- and *β*-CDs with Model Compounds. Before the formation of the side-chain hetero-polypseudorotaxane, we investigated the interaction of α- and *β*-CDs with model compounds (pC$_7$AMA and OEG-Azo in Scheme 1A,B) corresponding to the C$_7$ and Azo moieties in **1**, respectively, by ^{1}H NMR to estimate roughly apparent association constants (*K*) for each element.

Table 1. Association Constants (*K*) for α- and *β*-CDs with Model Compounds[a]

	$K \times 10^{-2}/M^{-1}$	
model compound	α-CD	*β*-CD
pC$_7$AMA	0.74	–[b]
OEG-*trans*-Azo	20	8.3
OEG-*cis*-Azo	0.21	5.0

[a] Determined by ^{1}H NMR assuming the formation of one-to-one complexes. [b] It was not possible to estimate the *K* because of no significant peak shifts.

Figure 1A shows an example of the ^{1}H NMR spectra for pC$_7$AMA in the presence of varying concentrations (C_{CD}) of α-CD. As C_{CD} is increased, small but clear downfield shifts and broadening of the signals due to the methylene protons in the C$_7$ side chain were observed, indicative of the interaction of α-CD with the C$_7$ side chain. Using the ^{1}H NMR spectra, the reciprocals of the peak shifts for the signal due to the proton (a) at 1.37 ppm in the C$_7$ moiety ($1/\Delta\delta_{obs}$) were calculated and plotted against the reciprocals of the α-CD concentrations ($1/C_{CD}$). As can be seen in Figure 1B, the plots show a good linear relationship, indicating that the interaction of α-CD with the C$_7$ moiety can be analyzed based on the formation of one-to-one complexes. From the intercept and the slope of the straight line, the *K* value was determined to be 7.4×10^1 M^{-1} by

$$\frac{1}{\Delta\delta_{obs}} = \frac{1}{K\Delta\delta C_{CD}} + \frac{1}{\Delta\delta} \quad (1)$$

where $\Delta\delta$ is the difference between the observed chemical shift for the one-to-one complex of α-CD with the C$_7$ moiety and the chemical shift in the absence of α-CD (Table 1). On the other hand, as can be seen in Figure S1, upon addition of 15.0 mM *β*-CD into the sample for pC$_7$AMA (1.0 mM in the C$_7$ moiety), the $\Delta\delta_{obs}$ value was so small that the *K* could not be estimated, indicative of only weak interaction of *β*-CD with the C$_7$ moiety.

Since this study utilizes the photoisomerization of the Azo moiety in OEG-Azo, the interaction of α- and *β*-CDs with the Azo moiety was investigated before and after the photoisomerization. Figure 2A,B shows examples of the ^{1}H NMR spectra of α- and *β*-CDs with OEG-Azo in the presence of varying CD concentrations before photoisomerization, in which most of the Azo moieties are in the *trans*-state. As can be seen in Figure 2A, all the signals due to the *trans*-Azo moiety shift to lower magnetic fields with increasing the α-CD concentration, indicative of the interaction of α-CD with the *trans*-Azo moiety. On the other hand, Figure 2B indicates that more complicated changes in the signals: the signals due to the protons (f and g) at 8.04 ppm in the Azo moiety show splitting and downfield shifts, and the signals due to the protons (h, i, and j) at 8.01 and 7.73 ppm exhibit broadening and upfield shifts with increasing the *β*-CD concentration. This observation indicates the interaction of *β*-CD with the *trans*-Azo moiety. Using the ^{1}H NMR spectra, the $1/\Delta\delta_{obs}$ values for the proton (f) in the *trans*-Azo moiety were calculated and plotted against $1/C_{CD}$. As can be seen in Figure 2C, the plots also show good linear relationships, indicating that the interaction of α- and *β*-CDs with the Azo moiety can be analyzed based on the formation of one-to-one complexes. Using eq 1, the *K* values were also estimated from the intercepts and the slopes of the straight lines to be 2.0×10^3 and 8.3×10^2 M^{-1} for α- and *β*-CDs, respectively, with the *trans*-Azo moiety in OEG-Azo (Table 1). Figure 3A,B shows examples of the ^{1}H NMR

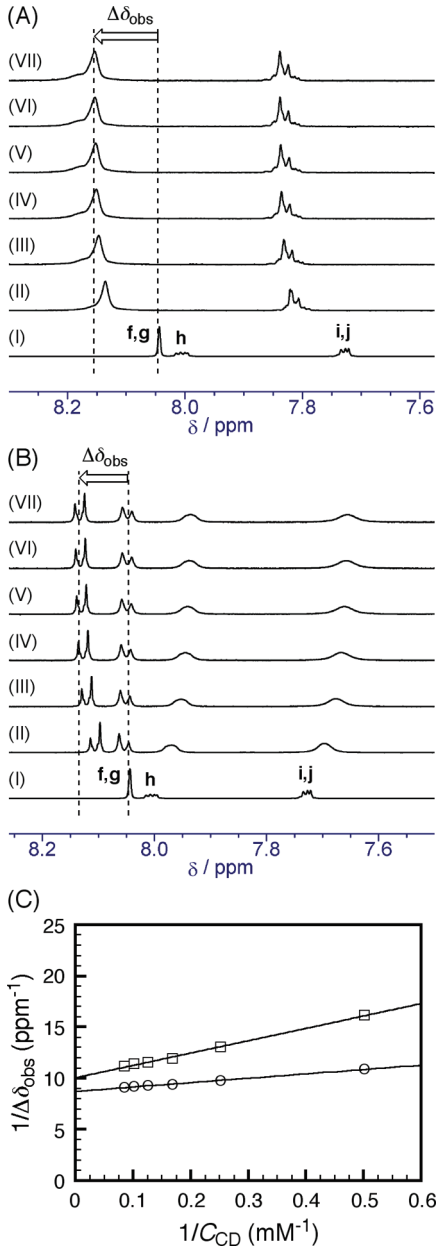

Figure 2. ^{1}H NMR spectra (A and B) of 1.0 mM OEG-*trans*-Azo (I) in the presence of various concentrations (C_{CD}) of α- and β-CDs measured in D_2O containing 5.0 mM $NaHCO_3$ and 5.0 mM Na_2CO_3 at 30 °C. C_{CD}: 0 (I), 2.0 (II), 4.0 (III), 6.0 (IV), 8.0 (V), 10.0 (VI), and 12.0 mM (VII). Benesi−Hildebrand plots (C) of $1/\Delta\delta_{obs}$ against $1/C_{CD}$ for OEG-*trans*-Azo with α- and β-CDs (circle and square, respectively).

spectra of α- and β-CDs with OEG-Azo in the presence of varying CD concentrations after irradiation with UV light (ca. 365 nm), in which more than 91% of the Azo moieties are in the *cis*-state for OEG-Azo and for the mixtures of OEG-Azo with α-CD and with β-CD. As shown in Figure 3A, the signals due to the protons (f and g) exhibit no significant changes, but slight downfield shifts for the signals due to the protons (h, i, and j) were observed with increasing the α-CD concentration, indicative of only weak interaction of α-CD with OEG-*cis*-Azo at the terminal of the *cis*-Azo moiety.[19] On the other hand, Figure 3B indicates the signals due to the protons (f, h, and j) at 7.78, 7.44, and 7.37 ppm exhibit downfield shifts and the signals due to the protons (g and i) at 7.12 and 7.05 ppm exhibit upfield shifts with increasing the β-CD concentration, indicative of the interaction of β-CD with the *cis*-Azo moiety in OEG-Azo. Using the ^{1}H NMR spectra, the $1/\Delta\delta_{obs}$ values of the protons (h and f) in the *cis*-Azo moiety for α- and β-CDs were calculated and plotted against $1/C_{CD}$ as can be seen in Figure 3C,D. Since these figures also show good linear relationships between $1/\Delta\delta_{obs}$ and $1/C_{CD}$, the K values were estimated using eq 1 with the intercepts and the slopes of the straight lines to be 2.1×10^1 and 5.0×10^2 M^{-1} for the complexation of α- and β-CDs with the *cis*-Azo moiety in OEG-Azo (Table 1).

Formation of Side-Chain Hetero-Polypseudorotaxane. On the basis of the K values for the complexation of α- and β-CDs with the model compounds (Table 1), we have prepared the side-chain hetero-polypseudorotaxane, in which α- and β-CDs include the C_7 and *cis*-Azo moieties, respectively. Figure 4 shows the synthetic scheme for the side-chain hetero-polypseudorotaxane. The structure of the polypseudorotaxane or polyrotaxane in each step has been characterized by cd and 2D NOESY NMR spectroscopies.

a. Formation of Side-Chain Polypseudorotaxane of ***1*** *and* α*-CD.* The first step is the formation of the side-chain polypseudorotaxane, in which α-CD includes the C_7 and *trans*-Azo moieties in the side chain, by adding α-CD to **1**. Since the apparent K (7.4×10^1 M^{-1}) for the complexation of α-CD with the C_7 moiety was not so high, excess α-CD was necessary. The α-CD concentration was fixed at 12.0 mM for **1** (1.0 mM in the C_7-OEG-Azo moiety), in which the peak shifts for the C_7 moiety in ^{1}H NMR were saturated as can be seen in Figure S2 of the Supporting Information.

Figure 5Ba shows the cd spectrum for the mixture of **1** and α-CD. This spectrum exhibits the negative and positive induced cd (icd) bands in the region of n−π* and π−π* transitions of the *trans*-Azo moiety, indicating that α-CD includes the *trans*-Azo moiety and the transition moments of n−π* and π−π* in the *trans*-Azo are perpendicular and parallel to the axis of the α-CD, respectively.[20] Figure 6 demonstrates the 2D NOESY NMR spectrum for the mixture of **1** and α-CD. This spectrum exhibits the correlation signals between the inner C3 and C5 protons in α-CD and the protons (f, g, h, i, and j) in the Azo moiety and between the C3 and C5 protons and the methylene proton (c) next neighboring the carbonyl group in the C_7 moiety. These data indicate that α-CD includes both the C_7 and Azo moieties, in which α-CD includes the Azo moiety from the primary hydroxy side because the correlation signals between the C3 and C5 protons and the protons (f, g, and h) in the Azo moiety are stronger than those between the C3 and C5 protons and the protons (i and j) in the Azo moiety. It should be noted that ^{1}H NMR for the mixture of **1** and α-CD exhibited a downfield shifted signal of methylene protons in the OEG linker, suggesting that some α-CD molecules were interlocked on the OEG linkers because excess α-CD was added. At present, however, we could not characterize how many α-CD molecules interlocked on the OEG linkers.

b. Formation of Side-Chain Polyrotaxane of ***1*** *and* α*-CD by Photoisomerization.* The second step is the formation of the side-chain polyrotaxane, in which α-CD is interlocked on the side chain by the *cis*-Azo stopper, by photoisomerization of the Azo moiety in the side-chain polypseudorotaxane prepared in the first step.[14,21,22]

We confirmed highly efficient *trans*-to-*cis* photoisomerization of the Azo moiety in **1** in the presence of 12.0 mM α-CD by UV−vis absorption and ^{1}H NMR spectroscopies. Figure 7 shows examples of the UV−vis absorption spectra for **1** (0.10 mM in the Azo moiety) in the absence (A) and presence (B) of 12.0 mM α-CD under photoirradiation. These figures demonstrate that the absorbances in the region of n−π* transition of the *trans*-Azo moiety gradually increase

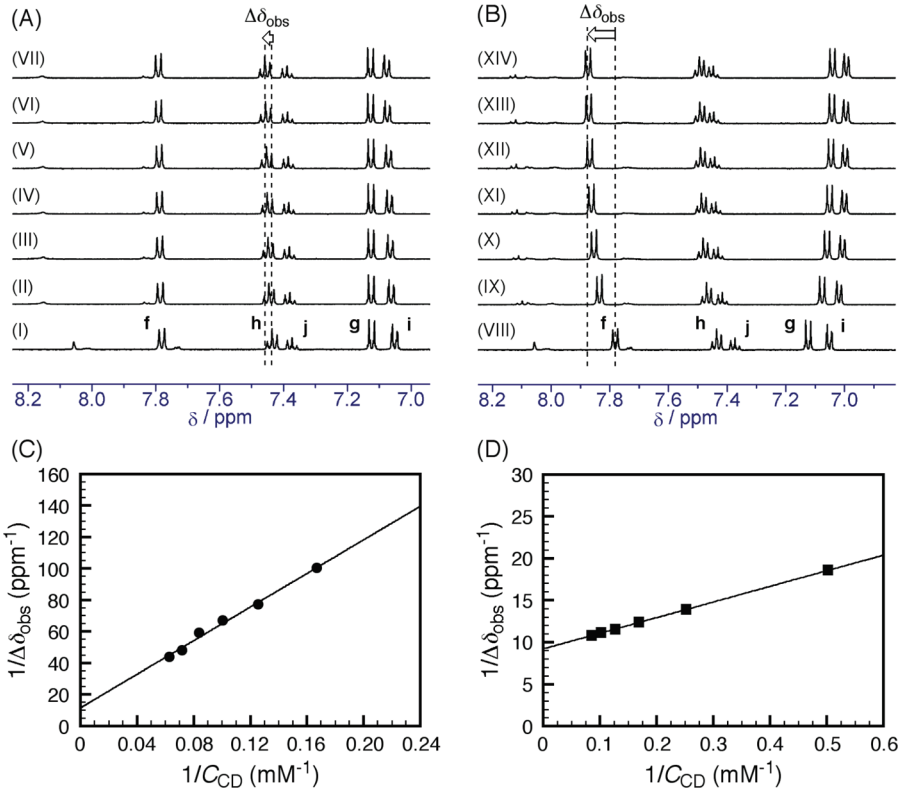

Figure 3. ^{1}H NMR spectra (A and B) of 1.0 mM OEG-*cis*-Azo (I and VIII) in the presence of various concentrations (C_{CD}) of α- and *β*-CDs measured in D_2O containing 5.0 mM $NaHCO_3$ and 5.0 mM Na_2CO_3 at 30 °C. C_{CD}: 0 (I and VIII), 2.0 (IX), 4.0 (X), 6.0 (II and XI), 8.0 (III and XII), 10.0 (IV and XIII), 12.0 (V and XIV), 14.0 (VI), and 16.0 mM (VII). Benesi−Hildebrand plots (C and D) of $1/\Delta\delta_{obs}$ against $1/C_{CD}$ for OEG-*cis*-Azo with α- and *β*-CDs (circle and square, respectively).

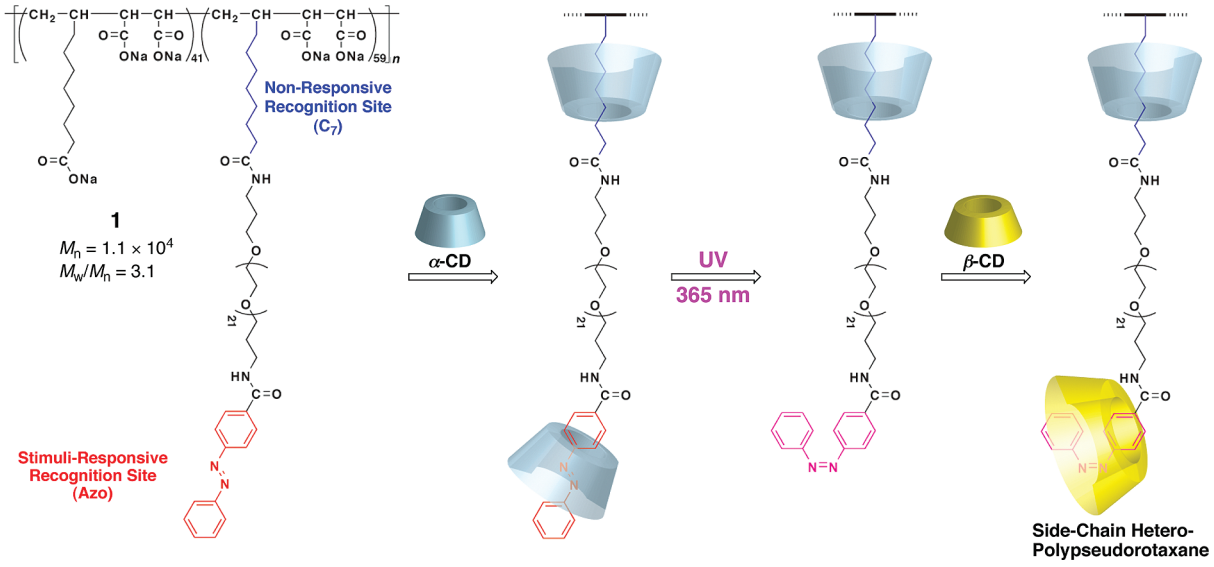

Figure 4. Synthetic scheme for the stepwise preparation of the side-chain hetero-polypseudorotaxane composed of α- and *β*-CDs.

with the irradiation time whereas those in the region of $\pi-\pi^*$ transition of the Azo moiety gradually decrease. Using the absorbances due to the Azo moiety at the initial state, at time t, and in the photostationary state (A_0, A_t, and A_{eq}, respectively) at 326.2 and 333.0 nm for **1** and for the mixture of **1** and α-CD, $\ln[(A_0 - A_{eq})/(A_t - A_{eq})]$ values were calculated and plotted against t as can be seen in Figure 7C. Since the plots show good linear relationships, the rate constants (k_t) of the *trans*-to-*cis* isomerization for the Azo moiety were estimated to be 3.9×10^{-2} and 4.9×10^{-2} s^{-1} for **1** and for the mixture of **1** and α-CD, respectively, from the slopes of the straight lines by

$$\ln \frac{A_0 - A_{eq}}{A_t - A_{eq}} = k_t t \qquad (2)$$

It should be noted here that the k_t value for the mixture of **1** and α-CD was larger than that for **1**. This may be because the Azo moieties in **1** somehow associate with each other and the complexation of α-CD dissociates the association of the Azo

moieties, resulting in a slight acceleration of photoisomerization.[23] ^{1}H NMR confirmed that the *cis*-Azo contents were as high as 85 and 91% for **1** and for the mixture of **1** and α-CD, respectively, in the photostationary state under irradiation with UV light (ca. 365 nm).

Figure 5Bb shows the cd spectrum for the mixture of **1** and α-CD after photoirradiation. This spectrum shows the very week icd bands ascribable to the residual *trans*-Azo complexed, indicative of almost no interaction of α-CD with the *cis*-Azo moiety. Figure 8 shows the 2D NOESY NMR spectrum for the mixture of **1** and α-CD after photoirradiation. This spectrum exhibits the correlation signals between the C3 and C5 protons in α-CD and the protons in the C_7 moiety whereas not between the C3 and C5 protons and the protons in the *cis*-Azo moiety, consistent with the *K* values of

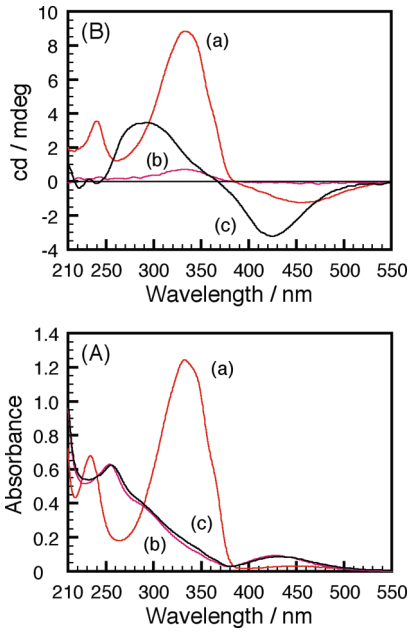

Figure 5. UV−vis (A) and cd (B) spectra of 0.10 mM **1** with 12.0 mM α-CD before (a) and after (b) photoirradiation (ca. 365 nm) and of 6.0 mM *β*-CD with the sample for *cis*-**1**/α-CD (c) measured in D_2O containing 5.0 mM $NaHCO_3$ and 5.0 mM Na_2CO_3 at 30 °C.

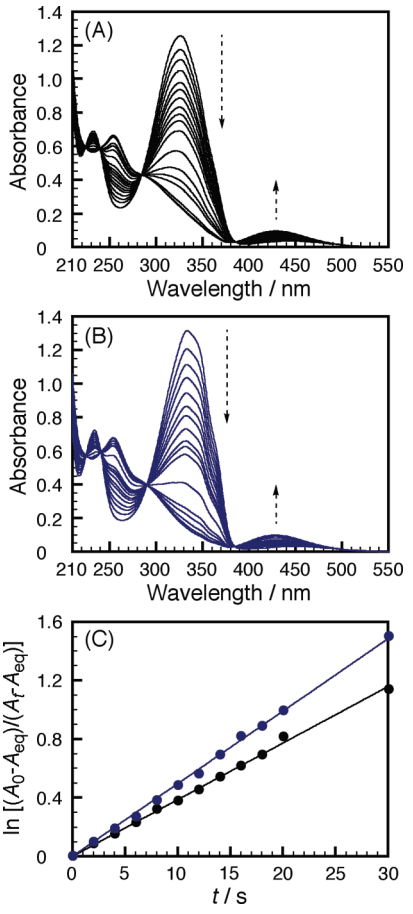

Figure 7. Time-dependent UV−vis spectra of 0.10 mM **1** in the absence (A) and presence (B) of 12.0 mM α-CD under irradiation with UV light (ca. 365 nm) measured in D_2O containing 5.0 mM $NaHCO_3$ and 5.0 mM Na_2CO_3 at 30 °C. The first-order plots (C) for *trans*-to-*cis* photoisomerization of **1** and of the mixture of **1** and 12.0 mM α-CD (black and blue circles, respectively).

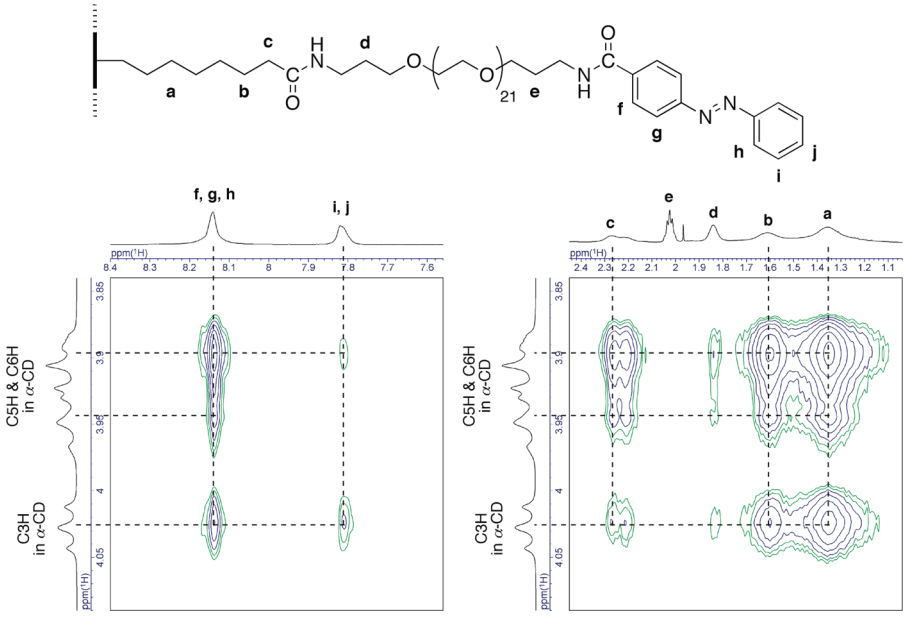

Figure 6. 2D NOESY NMR spectrum of 1.0 mM **1** with 12.0 mM α-CD measured in D_2O containing 5.0 mM $NaHCO_3$ and 5.0 mM Na_2CO_3 at 30 °C (τ_m = 200 ms).

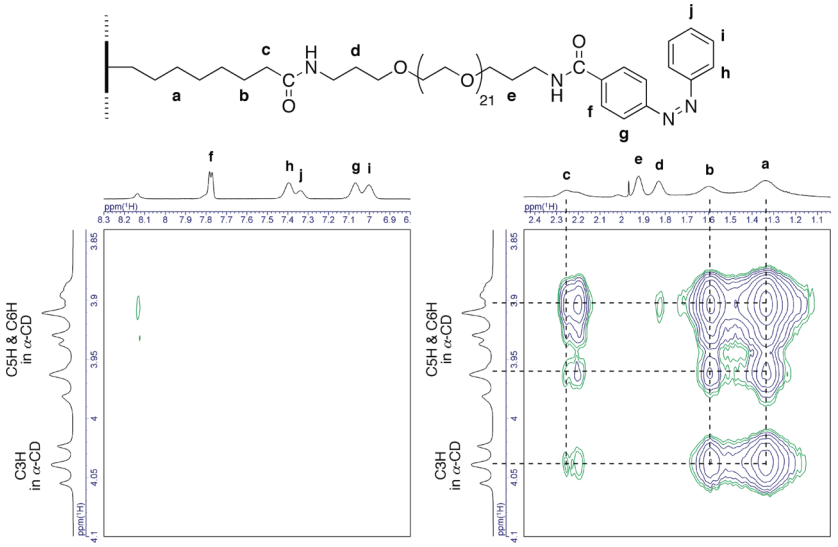

Figure 8. 2D NOESY NMR spectrum of the sample for 1.0 mM **1** with 12.0 mM α-CD after irradiation with UV light (ca. 365 nm) measured in D_2O containing 5.0 mM $NaHCO_3$ and 5.0 mM Na_2CO_3 at 30 °C (τ_m = 200 ms).

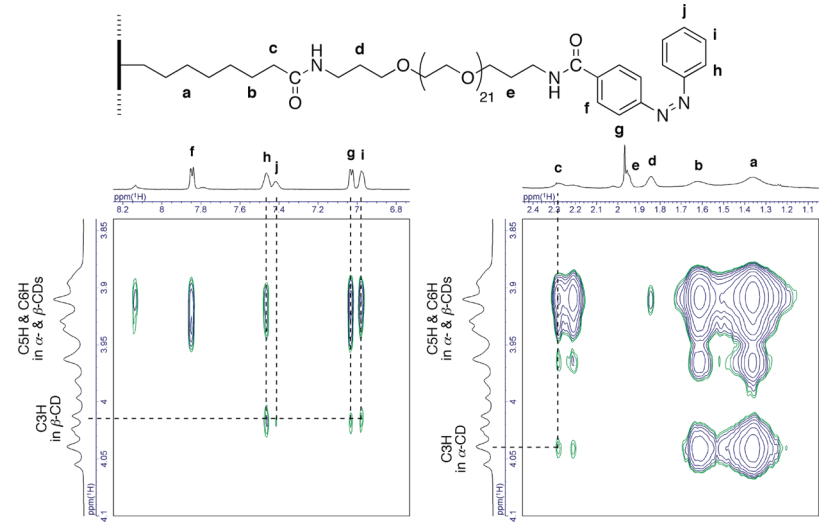

Figure 9. 2D NOESY NMR spectrum of 6.0 mM *β*-CD with the sample for *cis*-**1**/α-CD measured in D_2O containing 5.0 mM $NaHCO_3$ and 5.0 mM Na_2CO_3 at 30 °C (τ_m = 200 ms).

α-CD with pC_7AMA and OEG-*cis*-Azo (Table 1). It is noteworthy that the correlation signal between the C3 proton and the methylene proton (c) in the C_7 moiety is weaker than that between the C5 proton and the methylene proton (c) in the C_7 moiety, indicating that α-CD includes the C_7 moiety preferably from the secondary hydroxy side. These characterization data are indicative of the formation of the side-chain polyrotaxane, in which α-CD includes the C_7 moiety.[24]

c. Formation of Side-Chain Hetero-Polypseudorotaxane of cis-1/α-CD and β-CD. The final step is the formation of the side-chain hetero-polypseudorotaxane, in which *β*-CD includes the *cis*-Azo moiety at the end of the side chain, by adding *β*-CD to the side-chain polyrotaxane prepared in the second step. On the basis of K (5.0×10^2 M^{-1}) for the complexation of *β*-CD with the *cis*-Azo moiety, the *β*-CD concentration was fixed at 6.0 mM for the polyrotaxane of **1** and α-CD because the ^1H NMR signals for the inner C3 protons of α- and *β*-CDs significantly overlapped at concentrations >6.0 mM, as can be seen in Figure S3 of the Supporting Information.

Figure 5Bc indicates the cd spectrum for the mixture of *cis*-**1**/α-CD and *β*-CD. This spectrum shows the negative and positive icd bands in the region of n−π* and π−π* transitions of the *cis*-Azo moiety, indicating that *β*-CD includes the *cis*-Azo moiety and the transition moments of n−π* and π−π* in the *cis*-Azo are tilted to the axis of the *β*-CD.[20] Figure 9 shows the 2D NOESY NMR spectrum for the mixture of *cis*-**1**/α-CD and *β*-CD. This spectrum exhibits the correlation signals between the C3 proton in α-CD and the methylene proton (c) in the C_7 moiety and between the C3 proton in *β*-CD and the protons (g, h, i, and j) in the *cis*-Azo, agreeing with the K values listed in Table 1. The noteworthy is that no correlation signals were observed between the C3 proton in *β*-CD and the proton (f) in the *cis*-Azo and between the C5 proton in *β*-CD and the proton (j) in the *cis*-Azo, indicating that *β*-CD includes the *cis*-Azo moiety preferably from the primary hydroxy side. These characterization data confirmed the formation of the side-chain hetero-polypseudorotaxane, in which α- and *β*-CDs include the C_7 and *cis*-Azo moieties, respectively, as can be seen in Figure 4.[25]

Conclusion

We determined the K values for the complexation of α- and β-CDs with the model compounds (pC_7AMA, OEG-*trans*-Azo, and OEG-*cis*-Azo) by ^{1}H NMR. On the basis of the K values, we prepared the side-chain hetero-polypseudorotaxane from the water-soluble polymer (**1**) bearing C_7 and Azo moieties connected with OEG in the side chain, in which α- and β-CDs included the C_7 and *cis*-Azo moieties, respectively, by the three steps: (1) the formation of the side-chain polypseudorotaxane, in which α-CD included the C_7 and *trans*-Azo moieties in the side chain, (2) the formation of the side-chain polyrotaxane, in which α-CD was interlocked on the side chain by the *cis*-Azo stopper, by photoisomerization of the Azo moiety, and (3) the formation of the side-chain hetero-polypseudorotaxane, in which β-CD included the *cis*-Azo moiety at the end of the side chain. Each step was fully characterized by cd and 2D NOESY spectroscopies as well as the binding studies using model compounds. This system would be extended not only to contraction and expansion systems but also to nanotechnological applications such as nanodevices utilizing combinations of the host and guest polymers bearing CD and hydrophobic moieties, respectively, in their side chains.

Acknowledgment. The authors thank Mr. Seiji Adachi, Department of Chemistry, Graduate School of Science, Osaka University, for 2D NOESY NMR measurements. D.T. expresses his special thanks for The Global COE (Center of Excellence) Program "Global Education and Research Center for Bio-Environmental Chemistry" of Osaka University and for Japan Society of the Promotion of Science (JSPS) Research Fellowships for Young Scientists. This research is also supported in part by the CREST program of the JST.

Supporting Information Available: Figures showing ^{1}H NMR spectra of β-CD with pC_7AMA and those of α- and β-CDs with **1** before and after photoisomerization. This material is available free of charge via the Internet at http://pubs.acs.org.

References and Notes

(1) (a) Voet, D.; Voet, J. G. *Biochemistry*, 2nd ed.; Wiley & Sons: New York, 1995. (b) Stryer, L. *Biochemistry*, 4th ed.; W.H. Freeman: New York, 1995. (c) Alberts, B.; Johnson, A.; Lewis, J.; Raff, M.; Roberts, K.; Walter, P. *Molecular Biology of the Cell*, 4th ed.; Garland Science: New York, 2002.

(2) (a) Atwood, J. L.; Davies, J. E. D.; MacNicol, D. D.; Vögtle, F.; Lehn, J.-M. Supramolecular Technology. In *Comprehensive Supramolecular Chemistry*; Reinhoudt, D. N., Ed.; Pergamon: Oxford, UK, 1996; Vol. *10*. (b) Balzani, V.; Credi, A.; Raymo, F. M.; Stoddart, J. F. *Angew. Chem., Int. Ed.* **2000**, *39*, 3348–3391. (c) Balzani, V.; Credi, A.; Venturi, M. *Molecular Devices and Machines*, 2nd ed.; Wiley-VCH: Weinheim, 2008.

(3) (a) Sauvage, J.-P.; Dietrich-Buchecker, C. *Catenanes, Rotaxanes and Knots. A Journey Through the World of Molecular Topology*; Wiley-VCH: Weinheim, 1999. (b) Blanco, M.-J.; Jiménez-Molero, M. C.; Chambron, J.-C.; Heitz, V.; Linke, M.; Sauvage, J.-P. *Chem. Soc. Rev.* **1999**, *28*, 293–305. (c) Bonnet, S.; Collin, J.-P.; Koizumi, M.; Mobian, P.; Sauvage, J.-P. *Adv. Mater.* **2006**, *18*, 1239–1250.

(4) (a) Huang, T. J.; Brough, B.; Ho, C.-M.; Liu, Y.; Flood, A. H.; Bonvallet, P. A.; Tseng, H.-R.; Stoddart, J. F.; Baller, M.; Magonov, S. *Appl. Phys. Lett.* **2004**, *85*, 5391–5393. (b) Wu, J.; Leung, K. C.-F.; Benķtez, D.; Han, J.-Y.; Cantrill, S. J.; Fang, L.; Stoddart, J. F. *Angew. Chem., Int. Ed.* **2008**, *47*, 7470–7474.

(5) Coutrot, F.; Romuald, C.; Busseron, E. *Org. Lett.* **2008**, *10*, 3741–3744.

(6) (a) Badjic, J. D.; Balzani, V.; Credi, A.; Silvi, S.; Stoddart, J. F. *Science* **2004**, *303*, 1845–1849. (b) Badjic, J. D.; Ronconi, C. M.; Stoddart, J. F.; Balzani, V.; Silvi, S.; Credi, A. *J. Am. Chem. Soc.* **2006**, *128*, 1489–1499.

(7) Serreli, V.; Lee, C.-F.; Kay, E. R.; Leigh, D. A. *Nature* **2007**, *445*, 523–527.

(8) (a) Liu, Y.; Flood, A. H.; Bonvallet, P. A.; Vignon, S. A.; Northrop, B. H.; Tseng, H.-R.; Jeppesen, J. O.; Huang, T. J.; Brough, B.; Baller, M.; Magonov, S.; Solares, S. D.; Goddard, W. A.; Ho, C.-M.; Stoddart, J. F. *J. Am. Chem. Soc.* **2005**, *127*, 9745–9759. (b) Juluri, B. K.; Kumar, A. S.; Liu, Y.; Ye, T.; Yang, Y.-W.; Flood, A. H.; Fang, L.; Stoddart, J. F.; Weiss, P. S.; Huang, T. J. *ACS Nano* **2009**, *3*, 291–300. (c) Chuang, C.-J.; Li, W.-S.; Lai, C.-C.; Liu, Y.-H.; Peng, S.-M.; Chao, I.; Chiu, S.-H. *Org. Lett.* **2009**, *11*, 385–388.

(9) (a) Jiménez-Molero, M. C.; Dietrich-Buchecker, C.; Sauvage, J.-P. *Angew. Chem., Int. Ed.* **2000**, *39*, 3284–3287. (b) Jiménez-Molero, M. C.; Dietrich-Buchecker, C.; Sauvage, J.-P. *Chem.—Eur. J.* **2002**, *8*, 1456–1466. (c) Jiménez-Molero, M. C.; Dietrich-Buchecker, C.; Sauvage, J.-P. *Chem. Commun.* **2003**, 1613–1616.

(10) Fang, L.; Hmadeh, M.; Wu, J.; Olson, M. A.; Spruell, J. M.; Trabolsi, A.; Yang, Y.-W.; Elhabiri, M.; Albrecht-Gary, A.-M.; Stoddart, J. F. *J. Am. Chem. Soc.* **2009**, *131*, 7126–7134.

(11) Clark, P. G.; Day, M. W.; Grubbs, R. H. *J. Am. Chem. Soc.* **2009**, *131*, 13631–13633.

(12) Harada, A.; Hashidzume, A.; Yamaguchi, H.; Takashima, Y. *Chem. Rev.* **2009**, *109*, 5974–6023.

(13) (a) Harada, A.; Kamachi, M. *Macromolecules* **1990**, *23*, 2821–2823. (b) Harada, A.; Li, J.; Kamachi, M. *Nature* **1992**, *356*, 325–327. (c) Harada, A.; Li, J.; Kamachi, M. *Macromolecules* **1993**, *26*, 5698–5703.

(14) (a) Tomatsu, I.; Hashidzume, A.; Harada, A. *Angew. Chem., Int. Ed.* **2006**, *45*, 4605–4608. (b) Tomatsu, I.; Hashidzume, A.; Harada, A. *J. Am. Chem. Soc.* **2006**, *128*, 2226–2227.

(15) Tsukagoshi, S.; Miyawaki, A.; Takashima, Y.; Yamaguchi, H.; Harada, A. *Org. Lett.* **2007**, *9*, 1053–1055.

(16) (a) Tsuda, S.; Aso, Y.; Kaneda, T. *Chem. Commun.* **2006**, 3072–3074. (b) Dawson, R. E.; Lincoln, S. F.; Easton, C. *Chem. Commun.* **2008**, 3980–3982.

(17) Li, S.; Taura, D.; Hashidzume, A.; Takashima, Y.; Yamaguchi, H.; Harada, A., to be published.

(18) Koopmans, C.; Ritter, H. *J. Am. Chem. Soc.* **2007**, *129*, 3502–3503.

(19) (a) Cramer, F.; Hettler, H. *Naturwissenschaften* **1967**, *54*, 625–632. (b) Bortolus, P.; Monti, S. *J. Phys. Chem.* **1987**, *91*, 5046–5050.

(20) (a) Kodaka, M.; Fukaya, T. *Bull. Chem. Soc. Jpn.* **1989**, *62*, 1154–1157. (b) Kodaka, M. *J. Am. Chem. Soc.* **1993**, *115*, 3702–3705.

(21) (a) Born, M.; Ritter, H. *Makromol. Chem., Rapid Commun.* **1991**, *12*, 471–476. (b) Born, M.; Koch, T.; Ritter, H. *Acta Polym.* **1994**, *45*, 68–72. (c) Ritter, H. *Angew. Makromol. Chem.* **1994**, *223*, 165–175. (d) Born, M.; Ritter, H. *Angew. Chem., Int. Ed. Engl.* **1995**, *34*, 309–311. (e) Born, M.; Koch, T.; Ritter, H. *Macromol. Chem. Phys.* **1995**, *196*, 1761–1767. (f) Born, M.; Ritter, H. *Adv. Mater.* **1996**, *8*, 149–151. (g) Born, M.; Ritter, H. *Macromol. Rapid Commun.* **1996**, *17*, 197–202. (h) Noll, O.; Ritter, H. *Macromol. Rapid Commun.* **1997**, *18*, 53–58. (i) Sarvothaman, M. K.; Ritter, H. *Macromol. Rapid Commun.* **2004**, *25*, 1948–1952.

(22) Yamaguchi, I.; Osakada, K.; Yamamoto, T. *Macromolecules* **1997**, *30*, 4288–4294.

(23) Since the wavelength of the absorption maximum for **1** (λ_{max} = 326 nm) was practically the same as that (λ_{max} = 326 nm) for the model compound (OEG-Azo), it was difficult to discuss the aggregation of the *trans*-Azo moieties in **1** in the absence of α-CD from the UV−vis absorption spectra. However, we observed the NMR signals due to the Azo moieties in **1** became sharper upon addition of α-CD, indicative of association of the *trans*-Azo moieties in **1** in the absence of α-CD.

(24) It may be possible to isolate polyrotaxane of **1** with α-CD after photoisomerization by size exclusion chromatography or dialysis. However, it is known that the *cis*-Azo moiety is isomerized back to the *trans* isomer not only under visible light irradiation but also by a thermal process. Thus, we would not try to isolate the polyrotaxane by removing excess α-CD because we would like to maintain the *cis*-Azo content as high as possible.

(25) In this study, we used 12.0 mM α-CD and 6.0 mM β-CD for 1.0 mM C_7-OEG-Azo moieties in **1** because of ease of detail characterization. Using the association constants for the model compounds (Table 1), the mole fractions of the included C_7 and cis-Azo moieties were roughly estimated to be ca. 0.7 and 0.8, respectively, under the present conditions, indicating that the main species is the hetero-polypseudorotaxane.